



Microstructural evolution of the thermomechanically affected zone in a Ti–6Al–4V friction stir welded joint

L.H. Wu, D. Wang, B.L. Xiao and Z.Y. Ma*

Shenyang National Laboratory for Materials Science, Institute of Metal Research, Chinese Academy of Sciences,
72 Wenhua Road, Shenyang 110016, China

Received 20 December 2013; revised 16 January 2014; accepted 17 January 2014
Available online 25 January 2014

Microstructural evolution of the thermomechanically affected zone (TMAZ) in a friction stir welded Ti–6Al–4V joint was investigated by electron backscattered diffraction and transmission electron microscopy. The TMAZ showed the lowest hardness in the friction stir welded sample. By comparing microstructural details of the TMAZ, including texture, misorientation angle distribution and grain structure, with those of the base material, we propose a new grain refinement model associated with continuous dynamic recrystallization and grooving in the TMAZ.

© 2014 Acta Materialia Inc. Published by Elsevier Ltd. All rights reserved.

Keywords: Friction stir welding; Titanium alloys; Grain refinement; Recrystallization

Friction stir welding (FSW) is a relatively new solid-state joining technique, and has attracted great attention because of its advantages over conventional fusion welding techniques, such as higher joint efficiency, less distortion and lower residual stress [1]. FSW has been mainly applied to low melting temperature materials, such as Al and Mg alloys [2,3]. Recently, FSW of high melting temperature materials, such as Ti alloys, has attracted considerable interest [4]. Several studies indicated that high-quality defect-free Ti alloy welds could be obtained by FSW [5,6]. These results suggest that a more fundamental understanding of FSW processes of Ti alloys is needed in order to obtain the desired microstructure and properties.

It is well known that FSW or friction stir processing, when applied to aluminum alloys, generally produces three distinct regions: a stir zone (SZ), a thermomechanically affected zone (TMAZ) and a heat affected zone (HAZ). When they are applied to Ti alloys, however, there is some debate as to the existence of the TMAZ. Most of the early researchers [7,8] found no TMAZ in friction stir welded (FSWed) Ti alloy joints. Other researchers [9,10], however, observed a narrow TMAZ with obvious deformation characteristics in FSW/

friction stir processed (FSPed) Ti alloys by detailed microstructural observations.

Zhang et al. [7] found no TMAZ in FSWed Ti–6Al–4V joints and they attributed it to the phase transformation, which masked the deformation characteristic of the TMAZ. This explanation seems to be plausible for those alloys which experience allotropic transformation. The TMAZ was not obvious, however, even in those Ti alloys which did not experience allotropic transformation during FSW [11]. Therefore, the phase transformation may not be the intrinsic reason for the absence of the TMAZ in FSWed Ti alloy joints.

Knipling and Fonda [10] suggested that a narrow TMAZ could be attributed to the low thermal conductivity and abruptly changed the flow behavior of Ti alloys. The SZ (treated as a heat source) transferred a small amount of heat to the surrounding material, which only experienced a small temperature rise and therefore maintained a “hard” state. As a result, plastic deformation in the surrounding material was limited and a negligibly small TMAZ was produced. This explanation seems more plausible for various FSWed Ti alloy joints.

Although the TMAZ is negligibly small, clarifying the microstructural evolution in it is of great significance. On the one hand, because of its transitional nature, it is essential to understand how the original microstructure in the BM evolves into that in the SZ. On the other hand, this region may exhibit the lowest

* Corresponding author. Tel./fax: +86 24 83978908; e-mail: zyma@imr.ac.cn

hardness and thus become the failure position during the transverse tensile test of the weld. In this study, the lowest hardness was indeed observed in the TMAZ (Table 1).

In the past few years, the grain refinement mechanism in the TMAZ of FSWed/FSPed near- α and $\alpha + \beta$ Ti alloys has been investigated [2,10,12–14]. It was reported that, during FSW of near- α Ti-5111 alloy, the grain refinement mechanism in the TMAZ was continuous dynamic recrystallization (CDRX) related to shear-induced lattice rotation [10]. Ma et al. [2] proposed a similar CDRX mechanism in FSPed Ti-6Al-4V alloy. In most of these studies, however, fully lamellar structures were utilized as the base material (BM), and very few studies [13] have reported the grain refinement mechanism using other states, such as a mill-annealed state, as the BM.

Investigating the grain refinement mechanism using a mill-annealed BM is of significance from both scientific and engineering perspectives. First, plates or sheets with a mill-annealed state are mostly welded in industry. Second, the TMAZ is more difficult to identify in a mill-annealed BM compared to a fully lamellar BM, because an initial deformation feature may mask deformation characteristics in the TMAZ. The BM state was suggested to influence the grain refinement mechanism of the TMAZ [14].

Pilchak et al. [13] studied the microstructural evolution of the TMAZ of FSWed Ti-6Al-4V alloy using a mill-annealed BM, and suggested that the microstructural evolution of β phase in the TMAZ was dependent only on the temperature rise. Considering that the Ti-6Al-4V alloy contains two ductile phases which deform independently of each other, it is highly likely that the grain structure evolution of α phase is totally different from that of β phase. The grain refinement mechanism of α phase in the TMAZ of FSWed Ti-6Al-4V joints when using a mill-annealed BM is still far from fully understood, however, even though Ramirez and Juhas [14] succinctly reported that α grains were refined by DRX.

Therefore, the current study sought to elucidate the grain refinement mechanism of α phase in the TMAZ of the FSWed Ti-6Al-4V joint using a mill-annealed BM by electron backscattered diffraction (EBSD) and transmission electron microscopy (TEM), and a new grain refinement mechanism is proposed.

The as-received material was a 2.4-mm-thick mill-annealed Ti-6Al-4V sheet. The weld examined in this study was a bead-on-plate weld, which was produced at a rotation rate of 800 rpm and a transverse speed of 200 mm min⁻¹. A polycrystalline cubic boron nitride tool with a concave shoulder 15 mm in diameter and a triangular prism pin 6 mm in diameter and 2.2 mm in length was used. Argon shielding was employed to prevent the sheet surface from oxidizing.

In this work, the reference directions were selected as follows: RD, the rolling direction of the BM (i.e. the transverse direction of the FSWed sample); ND, the normal direction; and WD, the welding direction. The specimens for microstructural examinations were cross-sectioned perpendicular to the WD. Microstructural characterization was carried out by optical microscopy, EBSD and TEM. Specimens for both EBSD and TEM were prepared by twin-jet electropolishing with a solution of 6 vol.% HClO₄ + 34 vol.% CH₃OH + 60 vol.% C₄H₉OH at about -30 °C. EBSD maps were carried out at a step size of 0.1 μ m. Vickers hardness measurements were performed by applying a 100 g load for 15 s.

The transverse cross-sectional macrostructure of the FSWed Ti-6Al-4V joint is shown in Fig. 1. Three distinct regions can be detected: a bowl-shaped SZ, a BM and a narrow transition zone (<100 μ m in width). The latter region was assumed to be the TMAZ rather than HAZ because deformation characteristics were evident (which will be shown later).

The characteristic microstructural features of the BM and the TMAZ are shown in Fig. 2. The BM consisted of elongated α within subgrains, equiaxed α and a quite low volume fraction of residual β (black regions marked with white arrows), which were sporadically distributed between α grains (Fig. 2(a)). This suggests that partial recrystallization occurred in the BM. The average low and high angle grain boundary (LAGB, <15°, white line; HAGB, \geq 15°, black line) spacing of α grains in the ND was 1.1 and 1.8 μ m, respectively.

On the basis of its microstructural characterization, the TMAZ can be divided into TMAZ I and TMAZ II (Fig. 2(b)). In Fig. 2(b), the border of TMAZ II and SZ is marked according to whether or not the material exceeded β transus. The primary α in the TMAZ and a fully lamellar microstructure in the SZ suggest that the temperatures in these two regions were below and above the β transus, respectively (not shown).

In TMAZ I, a number of LAGBs were introduced to initial recrystallized α grains and therefore the large recrystallized grains were subdivided into smaller subgrains (Fig. 2(c)). Elongated α grains were fragmented and the elongated axis direction of the α grains deviated from the RD of the BM (Fig. 2(b)). When the strain further increased, in TMAZ II (Fig. 2(b)), the α grains were homogeneously refined to an average grain size of 0.8 μ m, which is even smaller than the subgrains in the BM, and slightly elongated along the border of the SZ and TMAZ II, which is the shear direction [12] (Fig. 2(d)). In other words, the grains in the TMAZ tended to align gradually along the shear direction.

The (0002) pole figure in Fig. 2(e) shows that the BM had a typical transverse basal texture with the maximum

Table 1. Vickers hardness of different zones of the FSWed Ti-6Al-4V joint (HV).

BM	TMAZ	SZ
369.4 ± 18.6	342.5 ± 9.5	357.6 ± 2.5

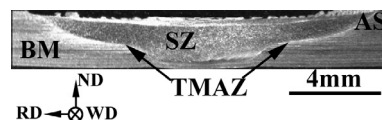


Figure 1. Optical cross-sectional macrograph of the FSWed Ti-6Al-4V joint.

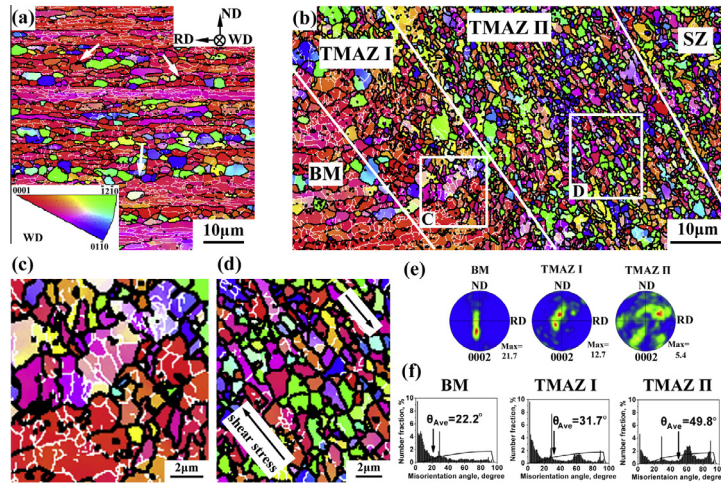


Figure 2. EBSD maps of (a) BM, (b) TMAZ, with selected areas shown at higher magnification in (c) and (d), (e) (0002) pole figure in the ND–RD reference frame and (f) misorientation angle distribution of BM and TMAZ (the curve denotes the random distribution for a hexagonal close-packed crystal). LAGBs and HAGBs are depicted by white and black lines, respectively.

intensity of ~ 21.7 times random at the location tilted $\sim 30^\circ$ from the WD towards the ND. From the BM to TMAZ II, the texture was randomized gradually (only ~ 5.4 times random in TMAZ II). The misorientation angle distributions in Fig. 2(f) indicate that the fraction of the HAGBs in the BM, TMAZ I and TMAZ II was 50.8%, 59.9% and 80.1%, respectively, and the average misorientation angle was 22.2° , 31.7° and 49.8° , respectively. The misorientation angle distribution from the BM to TMAZ II tended to match the random distribution. Therefore, α grains were homogeneously refined from the BM to TMAZ II, meanwhile the fraction of HAGBs and the average misorientation angle increased progressively; these are all features of CDRX. CDRX is related to relatively localized boundary migration, which usually occurs in high stacking fault energy metals, such as aluminum and beta titanium, during large deformation at high temperature. During CDRX, new grains are formed by the progressively increasing sub-grain boundary misorientation.

In order to further elucidate the grain refinement mechanism of the TMAZ, TEM examinations on the BM and the TMAZ were carried out (Fig. 3). The BM contained two different types of α grains: elongated grains within subgrains (Fig. 3(a)) and recrystallized grains with very few dislocations (Fig. 3(b)), attributed to partial recrystallization, as mentioned above. Very fine retained β phases were sporadically distributed between two α grains or at triple junctions (Fig. 3(a) and (b)).

In TMAZ I, adjacent to the BM, most α grains exhibited a deformation characteristic. Fig. 3(c) shows that, in TMAZ I, $\alpha \rightarrow \beta$ phase transformation occurred between two original elongated α grains, whereas β phase transformed into fine acicular $\alpha + \beta$ during the subsequent cooling. Grooves were observed across the α/α boundaries (white arrows in Fig. 3(c)), which was the result of a diffusional flux from β phase into the α/α boundaries owing to the equilibrium of various surface tension forces at triple junctions [15]. This process was obviously strongly dependent on temperature, and was beneficial for the fragmentation of α grains. For initial equiaxed recrystallized α grains, a large number of

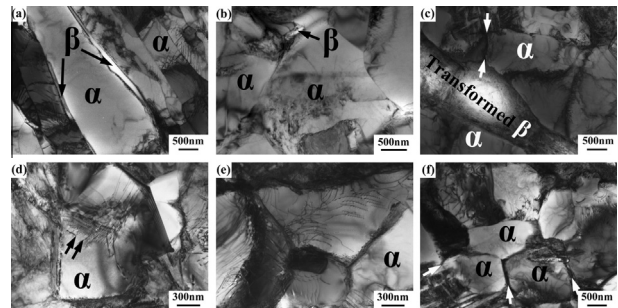


Figure 3. TEM micrographs showing grain structures of (a and b) BM, (c and d) TMAZ I and (e and f) TMAZ II: (a) elongated α grains, (b) coarse recrystallized α grains, (c) grooving across α/α boundaries, (d) dislocations in initial recrystallized α grains, (e) fragmented α grains and (f) refined equiaxed α grains.

dislocations were introduced (Fig. 3(d)). In some α grains, dislocations aligned to form subgrain boundaries (double arrows in Fig. 3(d)), which suggested the occurrence of dynamic recovery (DRV).

In TMAZ II, because of the higher temperature, a larger degree of β phase penetration occurred along the α/α subgrain boundaries and it broke up large α grains into several segments (Fig. 3(e)). In some places, a homogeneous microstructure with relatively equiaxed α grains was observed, which resulted from boundary splitting related to full penetration of β phase (Fig. 3(f)) [15]. Also, there were still a certain number of dislocations in these fragmented or equiaxed grains (Fig. 3(e) and (f)).

DRX generally softens the material, so the TMAZ showed a lower hardness than the BM. Also, generally speaking, an equiaxed microstructure shows a lower hardness than a fully lamellar microstructure for a given primary α grain size. Therefore, the TMAZ with an equiaxed microstructure showed the lowest hardness in the joint (Table 1).

From the analysis above, it can be concluded that α grain refinement should be related to CDRX. CDRX plays an important role during intermediate or high temperature deformation [16], and several mechanisms

related to CDRX have been proposed, including subgrain growth, lattice rotation, dislocation-absorbing and grain boundary sliding (GBS) [17].

In this study, GBS might be the main mechanism related to CDRX in the TMAZ because three features related to GBS could be observed in Fig. 2. First, it was suggested that a microstructure with fine grains promotes GBS [18]. GBS was reported in the SZ of an Al–Cu–Mg alloy with ultrafine grains during friction stir spot welding, where the strain rate was very high [19]. More recently, GBS was even reported to play an important role in pure Al with an average grain size of about 2 μm during deformation at room temperature [20]. The fine-grained microstructure in this study is believed to be beneficial for GBS (Fig. 2(a) and (b)). Second, the grains were slightly elongated in the direction of applied stress when GBS occurred [19], as can be seen in Fig. 2(d). Third, GBS favored texture and misorientation angle randomization [19,21], as shown in Fig. 2(e). Therefore, it is reasonable to infer that α/α GBS occurred during the grain refinement process in the TMAZ.

For two-phase Ti–6Al–4V alloy, the α/β interphase boundary also plays an important role during high temperature deformation in the two-phase region. It was reported that boundary sliding resistance follows the order $\alpha/\beta \ll \alpha/\alpha$ during superplastic deformation of Ti–6Al–4V [22], which means that α/β phase boundary sliding (PBS) occurs much more readily than α/α GBS. Therefore, in this study, PBS was likely to take place. $\alpha \rightarrow \beta$ phase transformation and grooving along the α/α boundaries in the TMAZ should favor PBS. Actually, GBS/PBS and grooving were not independent, but accelerated each other. The GBS/PBS helped the solute atoms around the boundaries to move faster, which accelerated grooving. At the same time, grooving made the α/β phase boundaries replace the α/α boundaries. Therefore, more PBS occurred, which caused α/α subgrains to rotate so as to achieve HAGBs [23]. Based on the discussion above, the following model is proposed to describe the evolution process of the α grain refinement in the TMAZ (Fig. 4):

1. Dislocation introduction and initial subgrain rotation by GBS (Fig. 4(a) and (b)). At the early stage of thermomechanical deformation, dislocations are introduced into α grains. Initial fine grains slide along the pre-existing grain boundaries, resulting in adjoining subgrain rotation to achieve HAGBs [24]. Also, limited grooving occurs because of the relatively low temperature.
2. DRV (Fig. 4(c)). In the subsequent thermomechanical cycle, dislocations arrange to form subgrain boundaries by DRV.

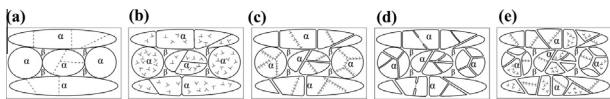


Figure 4. Schematic illustration of grain refinement process of TMAZ during FSW: (a) microstructure before deformation, (b) dislocation introduction, grooving and GBS, (c) dislocation arrangement and β penetration, (d) CDRX and (e) repetitive dislocation introduction and arrangement.

3. CDRX (Fig. 4(d)). At this stage, increased temperature results in the occurrence of more GBS/PBS and a faster grooving rate. Cooperation of GBS/PBS and grooving rapidly transforms the LAGBs of the new subgrains into HAGBs and thus CDRX occurs.
4. Repetitive dislocation introduction and arrangement (Fig. 4(e)). In the final thermomechanical deformation, dislocations are introduced in the refined recrystallized grains repeatedly and some of them arrange to form subgrain boundaries.

In summary, the grain refinement in the TMAZ of an FSWed Ti–6Al–4V joint was attributed to continuous dynamic recrystallization associated with subgrain rotation on the basis of dynamic recovery and grooving by β phase penetration. Grain and phase boundary sliding were the mechanisms of subgrain rotation.

This work was supported by the National Natural Science Foundation of China under Grant No. 51331008.

- [1] R.S. Mishra, Z.Y. Ma, *Mater. Sci. Eng. R* 50 (2005) 1.
- [2] Z.Y. Ma, A.L. Pilchak, M.C. Juhas, J.C. Williams, *Scripta Mater.* 58 (2008) 361.
- [3] J. Yang, D. Wang, B.L. Xiao, D.R. Ni, Z.Y. Ma, *Metall. Mater. Trans. A* 44A (2013) 517.
- [4] S. Mironov, Y. Zhang, Y.S. Sato, H. Kokawa, *Scripta Mater.* 59 (2008) 27.
- [5] L. Zhou, H.J. Liu, P. Liu, Q.W. Liu, *Scripta Mater.* 61 (2009) 596.
- [6] A.L. Pilchak, J.C. Williams, *Metall. Mater. Trans. A* 42A (2011) 1630.
- [7] Y. Zhang, Y.S. Sato, H. Kokawa, S.H.C. Park, S. Hirano, *Mater. Sci. Eng. A* 485 (2008) 448.
- [8] L. Zhou, H.J. Liu, Q.W. Liu, *J. Mater. Sci.* 45 (2010) 39.
- [9] A.L. Pilchak, M.C. Juhas, J.C. Williams, *Metall. Mater. Trans. A* 38A (2007) 401.
- [10] K.E. Knipling, R.W. Fonda, *Metall. Mater. Trans. A* 42A (2011) 2312.
- [11] A.P. Reynolds, E. Hood, W. Tang, *Scripta Mater.* 52 (2005) 491.
- [12] A.L. Pilchak, J.C. Williams, *Metall. Mater. Trans. A* 42A (2011) 773.
- [13] A.L. Pilchak, W. Tang, H. Sahiner, A.P. Reynolds, J.C. Williams, *Metall. Mater. Trans. A* 42A (2011) 745.
- [14] A.J. Ramirez, M.C. Juhas, *Mater. Sci. Forum* 426–4 (2003) 2999.
- [15] S. Zherebtsov, M. Murzinova, A. Salishchev, S.L. Sennatın, *Acta Mater.* 59 (2011) 4138.
- [16] A.H. Feng, Z.Y. Ma, *Acta Mater.* 57 (2009) 4248.
- [17] T.W. Nelson, J.Q. Su, R. Mishra, M. Mahoney, *Acta Mater.* 51 (2003) 713.
- [18] Z.Y. Ma, R.S. Mishra, M.W. Mahoney, *Acta Mater.* 50 (2002) 4419.
- [19] A.P. Gerlich, T. Shibayanagi, *Scripta Mater.* 60 (2009) 236.
- [20] K.V. Ivanov, E.V. Naydenkin, *Scripta Mater.* 66 (2012) 511.
- [21] M.T. Perez-Prado, G. Gonzalez-Doncel, O.A. Ruano, T.R. McNelley, *Acta Mater.* 49 (2001) 2259.
- [22] J.S. Kim, J.H. Kim, Y.T. Lee, C.G. Park, C.S. Lee, *Mater. Sci. Eng. A* 263 (1999) 272.
- [23] H.Q. Guo, C.X. Cao, L. Guo, H. Lin, *Rare Metal Mater. Eng. (Chinese ed.)* 38 (2009) 421.
- [24] H. Gudmundsson, D. Brooks, J.A. Wert, *Acta Metall. Mater.* 39 (1991) 19.